ELSEVIER

Journal of Chromatography A, 835 (1999) 169–185

JOURNAL OF CHROMATOGRAPHY A

Design of background electrolytes for indirect photometric detections based on a model of sample zone absorption in capillary electrophoresis

Xiang Xiong[a], Sam F.Y. Li[a,b,*]

[a]*Department of Chemistry, National University of Singapore, 10 Kent Ridge Crescent, Singapore 119260, Singapore*
[b]*Institute of Materials Research and Engineering, National University of Singapore, 10 Kent Ridge Crescent, Singapore 119260, Singapore*

Received 21 August 1998; received in revised form 2 December 1998; accepted 14 December 1998

Abstract

A unified model has been developed to describe the relationship between the sensitivity and the electrophoretic properties of the background electrolytes (BGEs). Five photometric detection methods for capillary electrophoresis (CE) have been discussed on the basis of the model. The results obtained show that the absorption of the sample zones in BGEs is a linear function of the transfer ratios of the sample ions, the molar absorptivities of the components of the BGEs and the sample ions, and the charge numbers of the ionic species involved in the sample zones. Simulation results indicate that the transfer ratios of the sample ions decrease with the increase of the mobilities of the sample ions in different BGEs. This suggests that the mobility of the co-ion in the BGE should be larger than or equal to that of the sample ions in order to increase the transfer ratios of the sample ions. Some rules extracted from the model show that the enhancement of the detection sensitivity lies in the maximization of the transfer ratios of the sample ions in the concerned BGEs and proper selection of the detection wavelength, but the constraints on the selection of the detection conditions are different for different detection methods. Experimental observations obtained are in good agreement with the simulation results. The model can be used as a guideline in formulation of BGEs for indirect photometric detections in CE.

Keywords: Background electrolyte composition; Photometric detection; Detection, electrophoresis; Inorganic anions; Inorganic cations; Organic acids

1. Introduction

Capillary electrophoresis (CE) is a separation process of charged species in a certain electrophoretic medium under a given electric field. The compositions of the electrophoretic media in CE fundamentally determine the migration behaviors of all individual analytes and very often also the detection sensitivity and separation selectivity. It is impossible to find one electrophoretic medium which can permit detection and separation of all charged molecules. Appropriate electrophoretic media should be designed when new separation problems are encountered in CE. Generally, a large number of compounds could be used as the components of the electrophoretic media; however, the selection of the

*Corresponding author.

0021-9673/99/$ – see front matter
PII: S0021-9673(98)01067-X

components of the electrophoretic media is not arbitrary. It is restricted by many factors, such as the detection modes (direct or indirect), the compatibility between the detection and separation conditions, buffer capacities, detection sensitivity and dynamic range [1], separation selectivity, matrix effects [2], etc. This makes the design of an electrophoretic medium for CE complicated because all these factors are not related explicitly.

Photometric detection is one of the detection schemes widely used in capillary zone electrophoresis (CZE) due to its easy accessibility in many laboratories and flexibility in operation. The majority of analytes with or without chromophores can be detected by using this approach. For analytes with chromophores, the detection of them is simply performed by recording the absorption of the sample ions themselves at the detector. Conversely, the detection of the analytes without chromophores is not based on recording the absorption of the sample ions directly, but on the decreases of the absorption of the sample zones, which are caused by the displacement of the chromophoric background electrolytes (BGEs) by the sample ions. In this case, the success of the detection of the analytes is largely dependent upon the proper formulation of the BGEs and selection of the detection conditions.

Models of absorption of sample zones play an important role in guiding the formulation of BGEs and enhancement of detection sensitivity. Several theoretical efforts towards this aspect have been reported [3–11]. The discussion was mainly based on the assumption of equivalent–per-equivalent displacement in a monovalent BGE (1:1) [12,13]. Although some rules have been deduced to guide the formulation of the BGEs for different classes of analytes [4,6,14], few models have been used to guide the design of BGEs for different detection methods [7]. The lack of a unified model to describe the absorption of sample zones in different BGEs leads to the formulation of BGEs for different detection methods being more practical than rational.

The purpose of this work is to develop a unified model, which characterises the absorption of the sample zones in BGEs based on interrelation of the electrophoretic and spectroscopic properties of the analytes and the components of the BGEs. Through interpretation of the model and simulation of the experiments, it is attempted to extract some guidelines and constraints to help the selection of the components of the BGEs and the evaluation of the performance of the BGEs for indirect photometric detections.

2. Model of sample zones absorption in BGEs

After sample injection, the ionic species in the sample plug will migrate to the detector, according to their intrinsic mobilities (superimposing electroosmotic flow in most cases), charges, and sizes, under the action of an electric field. Fig. 1 shows schematically the dynamic process of electrophoresis before a steady state of separation is reached. After a period of time (from time t_0 to t_4), the ionic species in the sample plug will be separated into individual zones which have sharp boundaries readily distinguishable by a detector. It should be noted that this separation result is generally obtained only under optimal conditions. At this baseline-separated state of the sample ions, the total concentration of the sample ions in the individual zones will remain constant though the peak shape may change with time because of diffusion. It is reasonable to assume that a steady state of separation has been reached at this moment and the following conditions should be satisfied for the sample zones and their adjacent BGE zones, namely,

1. The observed absorbance at a given wavelength is the summation of the contributions from all the

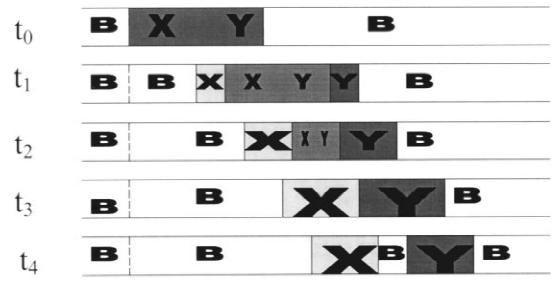

Fig. 1. Schematic diagram of the dynamic separation process after sample injection. Moment t_0 represents the initial state of separation after sample introduction. Moment t_4 represents the steady state of the electrophoretic separation. Moment t_1–t_3 represent the dynamic process of the separation of the analytes X and Y in the sample plug. B stands for BGE.

components in the individual zone and it obeys Beer's law, provided that the absorbance of the BGE is maintained within the linear range of the detector.

2. Electroneutrality is applicable in each of the zones.
3. Kohlrausch regulating function works throughout the electrophoresis process [15,16], provided that no sample overloading exists and the zones are adequately buffered [17–19].

If we suppose that the BGE is composed of a co-ion with $z_{\text{co-ion}}$ charge (absolute value, $z_{\text{co-ion}}>0$) and a counterion with $z_{\text{counterion}}$ charge (absolute value, $z_{\text{counterion}}>0$) as can be seen in Fig. 2A, at the steady state of electromigration of the BGE (i.e., the baseline-stabilized state) before sample injection, the following equations could be obtained by using the three conditions mentioned above, namely,

$$A^{\text{B}}_{\text{obs}} = A^{\text{B}}_{\text{co-ion}} + A^{\text{B}}_{\text{counterion}} \tag{1}$$

$$z_{\text{co-ion}}C^{\text{B}}_{\text{co-ion}} + [\text{H}^+] = z_{\text{counterion}}C^{\text{B}}_{\text{counterion}} + [\text{OH}^-] \tag{2}$$

$$\frac{z_{\text{co-ion}}C^{\text{B}}_{\text{co-ion}}}{\mu_{\text{co-ion}}} + \frac{z_{\text{counterion}}C^{\text{B}}_{\text{counterion}}}{\mu_{\text{counterion}}} = \text{const} \tag{3}$$

where superscript B and subscript obs denote the

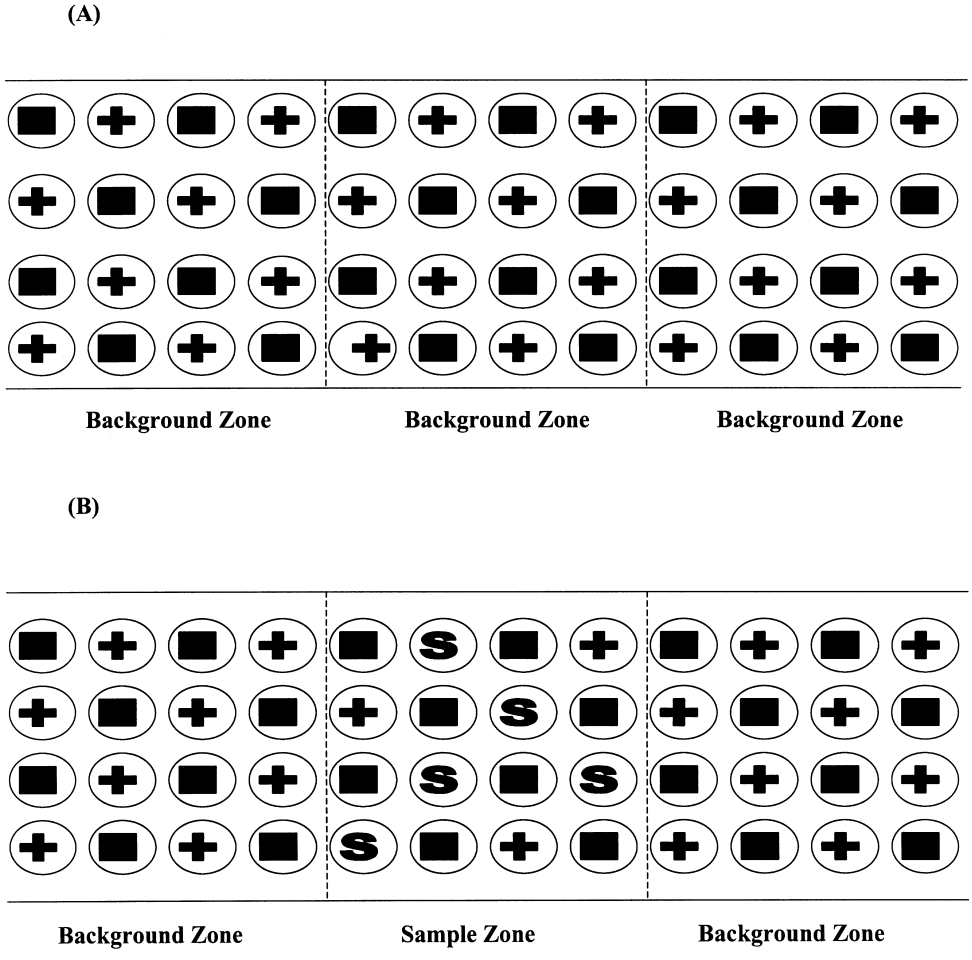

Fig. 2. Schematic representation of the zone composition at the steady state of separation before and after sample injection. (A) Before sample injection; (B) after sample injection. Symbol S denotes samples.

background electrolyte zone and the observed absorbance corresponding to this zone at the detector, respectively; C and μ refer to the concentrations of the components in the concerned zones and their effective mobilities (absolute value, $\mu>0$); A represents absorbance for any of the species in the zones. After sample injection, where the sample ions could be either cationic or anionic molecules with z_{sample} charge, and at the steady state of separation, the composition of the sample zones is schematically presented in Fig. 2B. Similarly, three other equations could be yielded for each of the sample zones, namely,

$$A^{\text{S}}_{\text{obs}} = A^{\text{S}}_{\text{co-ion}} + A^{\text{S}}_{\text{sample}} + A^{\text{S}}_{\text{counterion}} \tag{4}$$

$$z_{\text{co-ion}}C^{\text{S}}_{\text{co-ion}} + z_{\text{sample}}C^{\text{S}}_{\text{sample}} + [\text{H}^+] = z_{\text{counterion}}C^{\text{S}}_{\text{counterion}} + [\text{OH}^-] \tag{5}$$

$$\frac{z_{\text{co-ion}}C^{\text{S}}_{\text{co-ion}}}{\mu_{\text{co-ion}}} + \frac{z_{\text{sample}}C^{\text{S}}_{\text{sample}}}{\mu_{\text{sample}}} + \frac{z_{\text{counterion}}C^{\text{S}}_{\text{counterion}}}{\mu_{\text{counterion}}} = \text{const} \tag{6}$$

where superscript S represents the sample ion which always possesses the same sign of charge as that of the co-ion, i.e., either cationic or anionic species. For simplicity, cations are considered as the sample ions in the zones and the pH variation is neglected by assuming that the pH value within a zone is kept constant before and after sample injection at the baseline-separated state of the sample zones. By solving the six equations, we can obtain the change of absorbance in the individual sample zones, namely,

$$\Delta A = A^{\text{S}}_{\text{obs}} - A^{\text{B}}_{\text{obs}} = C^{\text{S}}_{\text{sample}} d \left[\varepsilon_{\text{sample}} - \text{TR} \cdot \varepsilon_{\text{co-ion}} + (z_{\text{sample}} - z_{\text{co-ion}} \cdot \text{TR}) \cdot \frac{\varepsilon_{\text{counterion}}}{z_{\text{counterion}}} \right] \tag{7}$$

with

$$\text{TR} = \frac{z_{\text{sample}}}{z_{\text{co-ion}}} \cdot \frac{\dfrac{\mu_{\text{counterion}}}{\mu_{\text{sample}}} + 1}{\dfrac{\mu_{\text{counterion}}}{\mu_{\text{co-ion}}} + 1} \tag{8}$$

where ε and d denote the molar absorptivities of the components in the zones at a given wavelength and the optical path length (i.e., the inside diameter of the capillary), respectively; TR is the transfer ratios of the sample ions which is defined as [20]

$$\text{TR} = \frac{C^{\text{B}}_{\text{co-ion}} - C^{\text{S}}_{\text{co-ion}}}{C^{\text{S}}_{\text{sample}}}$$

where the symbols have the meanings as above.

3. Experimental

3.1. Chemicals and solutions

All chemicals used in the present experiments were analytical grade or better. 4-Aminopyridine (>98%), benzylamine (>98%), *N*-phenylethylenediamine (>97%), pyromellitic acid (>97%) were obtained from Fluka (Buchs, Switzerland). 1,5-Naphthalenedisulfonic acid (>97%), sulfosalicylic acid (ACS reagent), and 1,2-dimethylimidazole (>98%) were purchased from Aldrich (Milwaukee, WI, USA). Tris (Electrophoresis purity) was obtained from Bio-Rad Labs. (Hercules, CA, USA). All solutions were prepared with Millipore water from a Milli-Q system (Millipore, Bedford, MA, USA). The stock solutions of standard analytes were prepared to ca. 1500 μg/mL by dissolving known amounts of each reagent in Millipore water. The model sample mixtures at μg/mL level were prepared daily by stepwise dilution of the standard stock solutions. The stock electrolyte solutions were prepared to be ca. 20 m*M* and the working electrolyte solutions were prepared by dilution from the stock solutions daily.

3.2. Apparatus

A laboratory-made capillary electrophoresis system, which consisted of a MicroUVIS 20 detector (Carlo Erba, Milan, Italy), a high voltage power supply (Spellman, Plainview, NY, USA), a DP700 data processor (Carlo Erba), and a fused silica capillary (Polymicro Technologies, Phoenix, AZ, USA), was used throughout the experiment. The dimensions of the capillary were 50 μm I.D.×358 μm O.D. The total length of the capillary was 44.0

cm with effective length of 38.0 cm. A pH meter (Model HANNA B417, Woonsocket, RI, USA) with ±0.01 pH resolution was used to measure the pH of the electrolyte solutions throughout the experiment. The UV–Vis spectra were obtained with a HP8452A diode array spectrophotometer (Hewlett-Packard, Waldbronn, Germany).

3.3. Capillary treatment

Each day, before sample injection, the capillary was rinsed with 1 *M* NaOH for half an hour, and then with 0.1 *M* NaOH for 15 min, followed by the running electrolyte solution for another half hour. After that, the capillary was washed by the running electrolyte under working voltage (29.0 kV) for 5–10 min until the baseline became stable. Through these treatments, the capillary was ready for use. No further washing of the capillary was performed in between sample injections unless a noisy baseline was observed. In the case of noisy baseline, the capillary was flushed with the running electrolyte solution for 4 or 5 times of the total volume of the capillary, and then washed by the running electrolyte solution under working voltage for several minutes until a stable baseline was reached. The results obtained showed that this treatment of capillary provided satisfactory reproducibility of the migration times with 0.7% RSD [with respect to electroosmotic flow (EOF)] for triplicate injections. The capillary was washed daily with water purified with a Millipore-Q system.

3.4. Procedures

All running electrolyte solutions were prepared daily by pipetting a certain volume of the organic base stock solution into a 15 mL bottle. The pH was adjusted with the organic acid to a specific pH value on the pH meter. Then the electrolyte solution was transferred to a 10 mL volumetric flask and diluted with Millipore water to the graduated marker. Prior to use, the running electrolyte solution was filtered through a 0.45 μm membrane filter (Phenomenex, Torrance, CA, USA), and then transferred to the two electrolyte reservoirs for separation. Indirect UV detection was carried out at 210 nm wavelength, unless otherwise stated, with reversal of the polarity of the signal output. The detector was located at the cathodic end of the capillary. Sample injections were performed hydrostatically at the anodic end of the capillary by raising the sample vial 19 cm above the level of the other/waste reservoir for 15 s. In between sample injections, approximately 30 s of standby time was adopted to minimize cumulative Joule heating effect.

3.5. Numerical analysis

Programs developed for the simulation of the different detection methods were written in Quick BASIC version 4.5 (Microsoft, Seattle, WA, USA). Results obtained were displayed by using Excel 97 (Microsoft, USA) which ran on Windows 95 environment.

4. Results and discussion

4.1. Absorption of sample zones in BGEs for different detection methods

Based on Eq. (7), four indirect photometric detection methods can be designed as follows:

1. the co-ion having UV absorption, the counterion being non-UV absorbing;
2. the counterion having UV absorption, the co-ion being non-UV absorbing;
3. both the co-ion and the counterion having UV absorption, but detection is carried out at a single wavelength;
4. both the co-ion and the counterion having UV absorption, but detection is carried out at dual wavelengths.

The first detection method has been employed in many practical applications [20,21], but the other three methods have been described in only a few reports [22–24]. By assuming appropriate parameters in Eq. (7), the expressions for the absorption of the sample zones in BGEs for the different detection methods could be obtained individually as given in Table 1, where the sample ions were discriminated by being UV absorbing ($\varepsilon_{\text{sample}} > 0$) or non-UV absorbing ($\varepsilon_{\text{sample}} = 0$). From Table 1 we can see that the absorbances of the sample zones are linear functions of the transfer ratios of the sample ions, the

Table 1
Absorbances of sample zones in BGEs under different modes of photometric detection

Detection mode of photometry	Absorbances of sample zones in BGEs	
	$\varepsilon_{sample} > 0$	$\varepsilon_{sample} = 0$
(I) Indirect		
(1) Co-ion having UV absorption $\varepsilon_{co\text{-}ion} > 0$ $\varepsilon_{counterion} = 0$	$C^s_{sample} d(\varepsilon_{sample} - TR \cdot \varepsilon_{co\text{-}ion})$	$-C^s_{sample} d \cdot TR \cdot \varepsilon_{co\text{-}ion}$
(2) Counterion having UV absorption $\varepsilon_{co\text{-}ion} = 0$ $\varepsilon_{counterion} > 0$	$C^s_{sample} d[\varepsilon_{sample} + (z_{sample} - z_{co\text{-}ion} \cdot TR)\varepsilon_{counterion}/z_{counterion}]$	$C^s_{sample} d(z_{sample} - z_{co\text{-}ion} \cdot TR)\varepsilon_{counterion}/z_{counterion}$
(3) Binary UV absorption with single detection wavelength $\varepsilon_{co\text{-}ion} > 0$ $\varepsilon_{counterion} > 0$	$C^s_{sample} d[\varepsilon_{sample} - TR \cdot \varepsilon_{co\text{-}ion} + (z_{sample} - z_{co\text{-}ion} \cdot TR) \varepsilon_{counterion}/z_{counterion}]$	$C^s_{sample} d[-TR \cdot \varepsilon_{co\text{-}ion} + (z_{sample} - z_{co\text{-}ion} \cdot TR) \cdot \varepsilon_{counterion}/z_{counterion}]$
(4) Binary UV absorption with dual detection wavelength $\varepsilon_{co\text{-}ion} > 0$[a] $\varepsilon_{counterion} \cong 0$	$C^s_{sample} d(\varepsilon_{sample} - TR \cdot \varepsilon_{co\text{-}ion})$	$-C^s_{sample} d \cdot TR \cdot \varepsilon_{co\text{-}ion}$
(II) Direct		
(5) Non-UV absorption BGE $\varepsilon_{co\text{-}ion} = 0$ $\varepsilon_{counterion} = 0$	$C^s_{sample} d \varepsilon_{sample}$	0

[a]Here, co-ion refers to either cationic or anionic components of the BGEs where they are applicable.

molar absorptivities of the components of the BGEs and the sample ions, and the charge numbers of the ionic species involved in the sample zones. The complexity of the equations is different for different detection methods. This suggests that the proper formulation of the BGEs and enhancement of the detection sensitivity have their inherent criteria for different detection methods. In particular, the explicit relationships between the properties of the components of the BGEs and the absorbances of the sample zones are not directly recognizable for detection methods 2 to 4. Further reduction of these equations is needed to disclose the inherent relationships between all the parameters involved.

4.2. Transfer ratios of sample ions in different BGEs

It should be pointed out that the parameter TR is involved in all the equations in Table 1. This means that judicious control of the transfer ratio would greatly affect the detection sensitivity and the dynamic range of quantitation. However, little is known about the transfer ratios of sample ions in different BGEs [13]. From Eq. (8), we can know that the transfer ratios consist of two parts. One is the charge ratio of the sample ion to the co-ion; the other is the degree of mobility match (DMM) between the sample ion and the co-ion in a given BGE, namely,

$$TR = \frac{z_{sample}}{z_{co\text{-}ion}} \cdot DMM$$

with

$$DMM = \frac{\frac{\mu_{counterion}}{\mu_{sample}} + 1}{\frac{\mu_{counterion}}{\mu_{co\text{-}ion}} + 1} \quad (9)$$

As a result, the magnitude of the transfer ratio of a sample ion is dependent on the charge numbers and

Table 2
Three cases of combination of BGEs in terms of mobilities of the co-ion and the counterion

Case of combination of BGE	Mobility (10^{-5} cm^2 V^{-1} s^{-1})	
	Co-ion	Counterion
Case 1		
$\mu_{co\text{-}ion} < \mu_{counterion}$	50	70
Case 2		
$\mu_{co\text{-}ion} = \mu_{counterion}$	50	50
Case 3		
$\mu_{co\text{-}ion} > \mu_{counterion}$	50	20

the electrophoretic properties of the sample ions and the components of the BGEs. Generally, only three cases of combination of BGEs in terms of the mobilities of the co-ions and the counterions are encountered in capillary electrophoresis. These combinations are presented in Table 2 with the assumption of the values of mobilities for the co-ion and the counterion. Fig. 3 shows the simulation results of the transfer ratios of the sample ions with different charge ratios of samples to co-ions in the three cases of BGEs as given in Table 2. From Fig. 3 we can see that case 3 is the less favourable combination due to its lower transfer ratios for the sample ions as compared with the other two cases. In addition, the transfer ratios decrease for all three cases with respect to the charge ratios as the mobilities of the sample ions increase. The larger the charge ratio of the sample ion to the co-ion, the greater the transfer ratio of the sample ion is. Sample ions with their mobilities larger than that of the co-ion have lower transfer ratios, while the sample ions with their mobilities equal to or less than that of the co-ion have larger transfer ratios. Moreover, the transfer ratios of the sample ions are only dependent upon the degree of mobility match in a given BGE when the charge ratios of the sample ions to the co-ions are unity as can be seen in Fig. 3. From these simulation results, it can be inferred that the co-ion with the largest mobility (compared to the mobilities of the sample ions) would maximize the transfer ratios of the sample ions and enhance the sensitivity

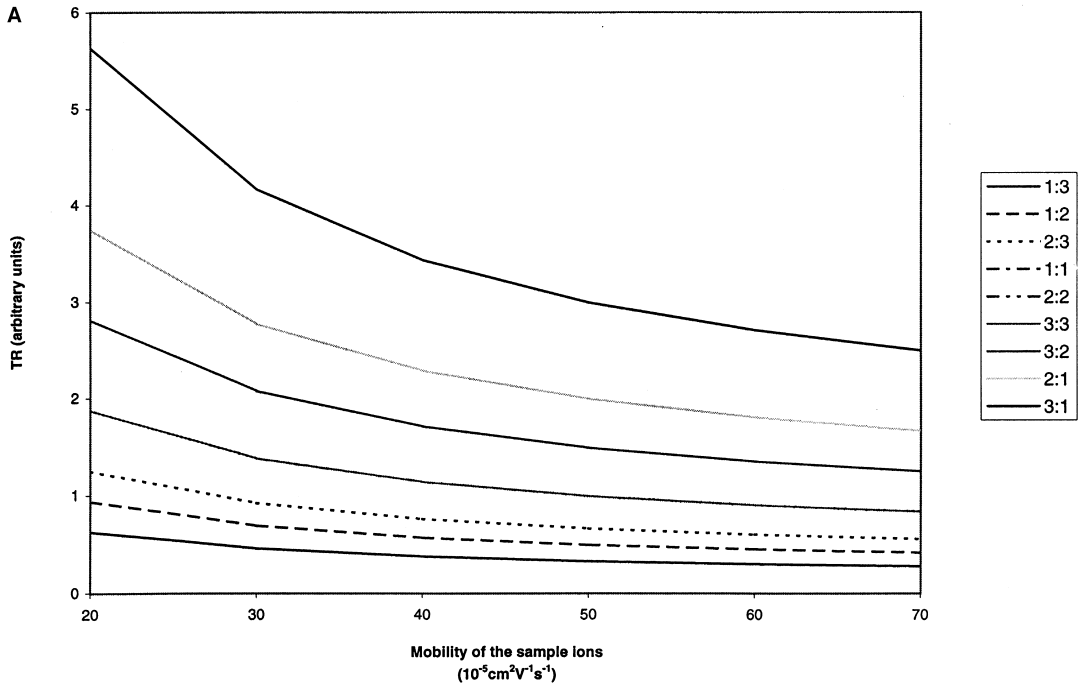

Fig. 3. Transfer ratios of sample ions in different BGEs. (A) Case 1 combination of BGE; (B) Case 2 combination of BGE; (C) Case 3 combination of BGE. The relevant parameters of the BGEs are given in Table 2. Charge ratios of sample ions to co-ions ($z_{sample}/z_{co\text{-}ion}$) are labelled in the figure. When the $z_{sample}/z_{co\text{-}ion}$ equals one, the TR curves for the sample ions overlap.

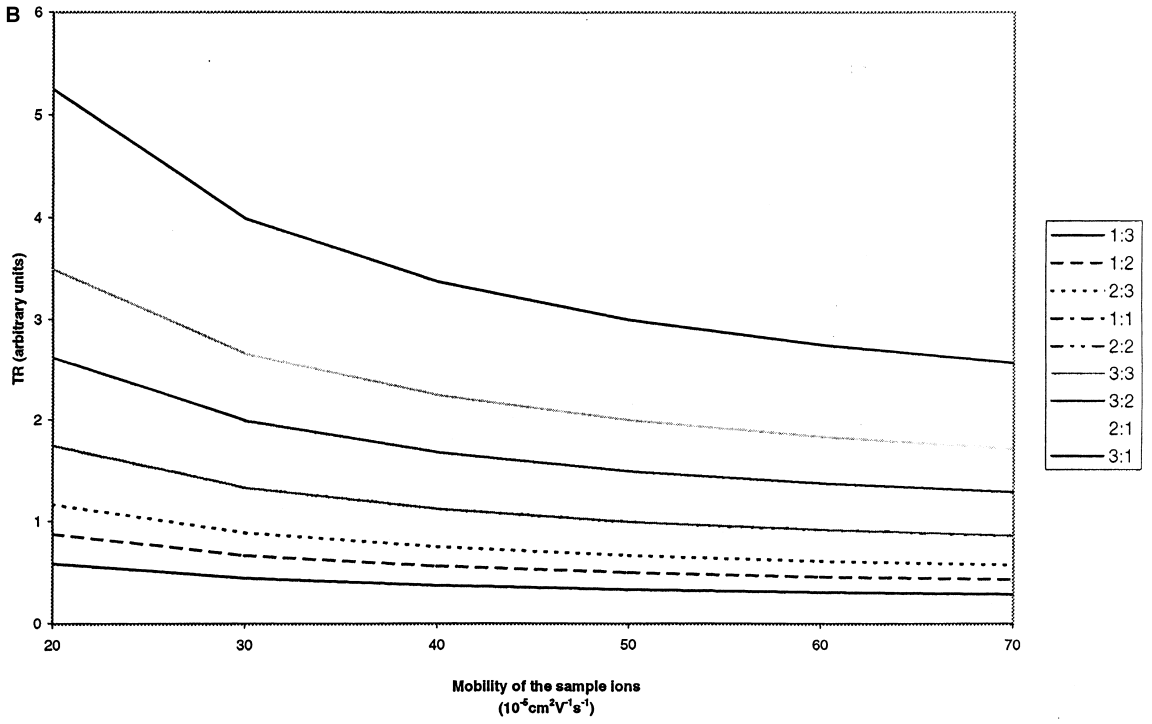

Fig. 3. (*continued*)

of the detection. However, great mismatch of mobilities between the co-ion and the sample ions would give rise to very distorted peaks due to excessive electromigration dispersion [11]. Practically, BGEs with their mobilities matched well to the interested sample ions were the desirable choice by compromising the transfer ratios, peak shape and resolution.

4.3. Detection constraints for indirect photometric methods

4.3.1. Method 1

From Table 1, we can see that the absorption of the sample ions themselves always offset the signal intensity observed at the detector. When the detection wavelength is selected at which sample ions have strong absorption, the sensitivity obtained for these sample ions would be lower than those without absorption at the same wavelength. For simplicity, sample ions without photometric absorption, i.e., $\varepsilon_{\text{sample}} = 0$, were used to evaluate the equation derived. Fig. 4 shows the peak height of three alkali metals in different BGEs. Table 3 gives the electrophoretic and spectroscopic properties of some cationic and anionic components of BGEs used in the present work. By comparing Figs. 3 and 4, we can see that the peak height decreases with the increase of the effective mobilities of the sample ions, and that the magnitude of the peak height of the alkali metals in the three BGEs follows the order: 4-aminopyridine > benzylamine > *N*-phenylethylenediamine. This observation is in good agreement with the magnitude of the transfer ratios estimated and molar absorptivities of the three BGEs as given in Table 3. Similar phenomena have also been observed for several anionic ions in sulfosalicylic acid/Tris and nicotinic acid/Tris BGEs [28]. This indicates that transfer ratios and molar absorptivities of the BGEs are the key factors dictating the sensitivity of detection for this method except the effect of electromigration dispersion of the peaks [11].

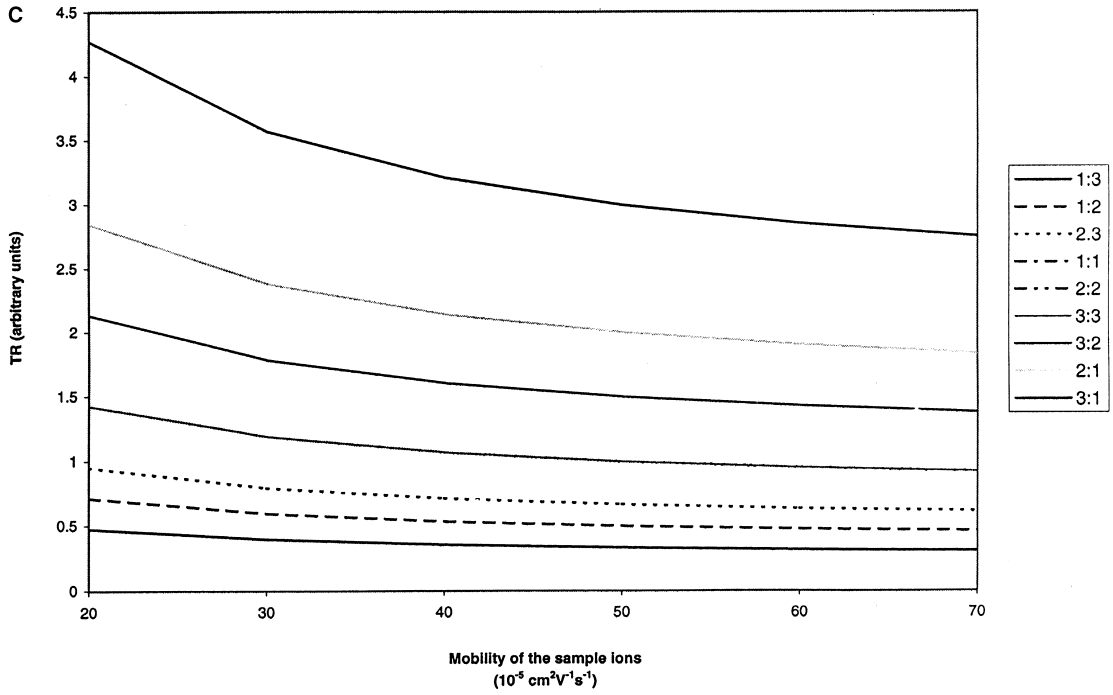

Fig. 3. (*continued*)

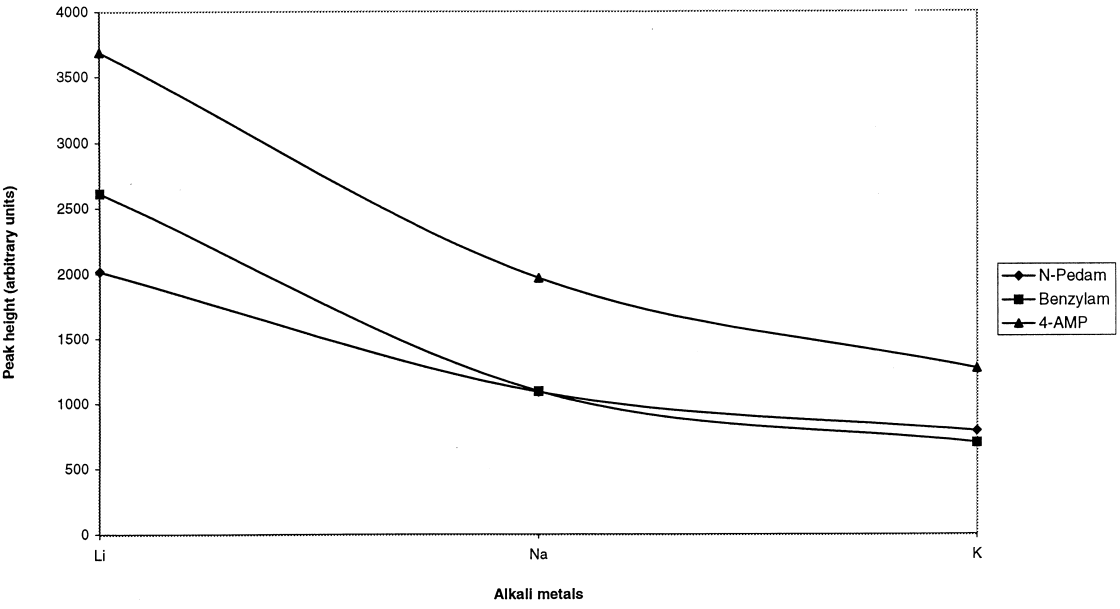

Fig. 4. Peak height of some alkali metals in different BGEs. BGEs of 6 m*M* 4-aminopyridine (4-AMP), benzylamine (Benzylam), and *N*-phenylethylenediamine (Pedam) with sulfuric acid adjusting pH, respectively. pH = 4.0; λ = 210 nm; V = 15.0 kV; concentrations for each of the sample ions are 20 μg/mL. RSD for the peak height measurement ranges from 1.5–6%.

Table 3
Electrophoretic and spectroscopic properties of some cationic and anionic compounds of BGEs used in the present work

Components of BGE	pK_a [27]	Molar absorptivity[a] (mol^{-1} cm^{-1} L)	Effective mobility[b] (10^{-5} cm^2 V^{-1} s^{-1})
Cationic			
4-Aminopyridine	9.11	$1.6 \cdot 10^4$ (210 nm)	43
Benzylamine	9.35	$7.2 \cdot 10^3$ (210 nm)	35
N-phenylethylenediamine [25]	6.70 (pK_1)	$7.1 \cdot 10^3$ (210 nm)	30
	9.80 (pK_2)		
1,2-dimethylimidazole [26]	8.21	$6.4 \cdot 10^3$ (210 nm)	23
		$5.2 \cdot 10^3$ (217 nm)	
		$1.9 \cdot 10^3$ (226 nm)	
Anionic			
1,5-Naphthalenedisulfonic acid	N/A[c]	$8.9 \cdot 10^4$ (224 nm)	−74
Sulfosalicylic acid	2.49 (pK_1)	$4.4 \cdot 10^4$ (210 nm)	−84
	12.00 (pK_2)	$2.2 \cdot 10^4$ (217 nm)	
		$9.2 \cdot 10^3$ (226 nm)	
Pyromellitic acid	1.92 (pK_1)	$2.4 \cdot 10^4$ (210 nm)	−100
	2.87 (pK_2)		
	4.49 (pK_3)		
	5.63 (pK_4)		

[a]The molar absorptivities of the compounds were obtained by plotting absorbance against concentration with correlation coefficients being larger than 0.99.
[b]The effective mobilities of the compounds were calculated by using the migration time determined in 6.75 mM phosphate buffer with RSD ranging from 0.4 to 2.4%. pH = 7.7, λ = 210 nm, the neutral marker used to determine the EOF was benzyl alcohol. Other conditions see the experimental section.
[c]Data is unavailable.

4.3.2. Method 2

From the equation for this method in Table 1, it is not easy to identify how BGEs influence the absorption of the sample zones. Further reduction of the equation is necessary. For simplicity, the sample ions are considered as being photometrically non-absorptive, i.e., $\varepsilon_{\text{sample}} = 0$. By using Eq. (9), the absorption of the sample zones for this detection method can be reduced to

$$\Delta A = A^{\text{S}}_{\text{obs}} - A^{\text{B}}_{\text{obs}} = C^{\text{S}}_{\text{sample}} d(1 - \text{DMM}) \cdot \frac{z_{\text{sample}}}{z_{\text{counterion}}} \cdot \varepsilon_{\text{counterion}} \quad (10)$$

where all the symbols have the same meanings as before. Because of the difference in compositions of BGEs, three cases of absorption for the sample zones would be observed, i.e.,

$\Delta A = A^{\text{S}}_{\text{obs}} - A^{\text{B}}_{\text{obs}} < 0$ (normal displacement)

$\Delta A = A^{\text{S}}_{\text{obs}} - A^{\text{B}}_{\text{obs}} = 0$ (no peak)

$\Delta A = A^{\text{S}}_{\text{obs}} - A^{\text{B}}_{\text{obs}} > 0$ (positive peak, absorbance increase)

If it is assumed that the molar absorptivities of the counterions and the charges of the sample ions and the counterions are all positive numbers, then the detectability of the sample ions is only dependent on the third term in Eq. (10). Fig. 5 shows the relationship between (1 − DMM) and the mobilities of the sample ions in different BGEs as listed in Table 2. By comparing Fig. 5 with Table 2, we can see that sample ions with mobilities less than those of the co-ions would be detected as a normal displacement peak. Positive peaks would be observed at the detector for the sample ions having larger mobilities than that of the co-ion, but no peaks would be detected when the mobilities of the samples were equal to that of the co-ion. These phenomena have been observed for some cationic analytes in BGEs of benzoic acid with NaOH and KOH adjusted pH,

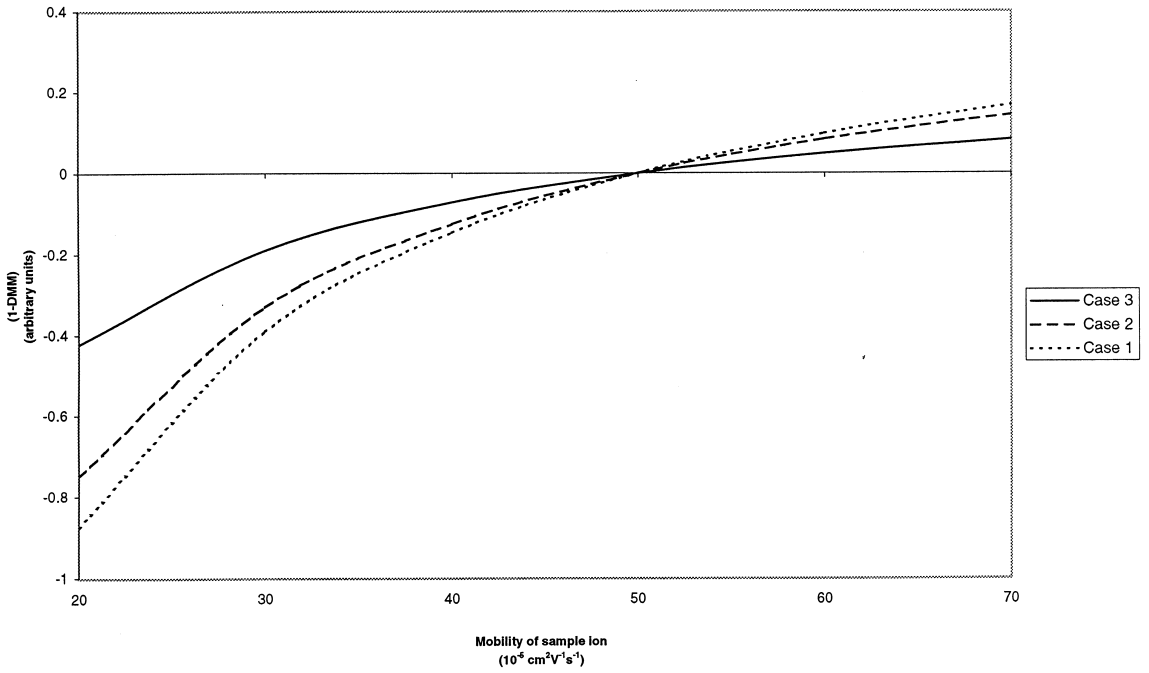

Fig. 5. Plot of (1−DMM) against the effective mobilities of the sample ions in different BGEs (as given in Table 2).

respectively, and BGEs of *p*-anisic acid with Tris and ethanolamine adjusted pH, respectively [7]. Fig. 6 shows the simultaneous detection of three cations and six anions in Tris/1,5-naphthalenedisulfonic acid BGE. The cations were detected as positive peaks because their mobilities were larger than that of their co-ion (Tris), while the anions were detected as negative peaks because the anions were detected on the basis of normal displacement of their co-ion (1,5-naphthalenedisulfonate). The co-ions and the counterions are different for different analytes. For cationic analytes, Tris is the co-ion and 1,5-naphthalenedisulfonate is the counterion. For anionic analytes, the reverse is applicable. Because of the complexity of the electropherograms for this method, the applications of it are very limited [29].

4.3.3. Method 3

Because both the co-ion and the counterion are photometrically absorptive, the proper selection of the detection wavelength is critical for the successful detection of the various sample ions. By using Eq. (9), the absorption of the sample zones for this detection method can be expressed as

$$\begin{aligned}\Delta A &= A^{S}_{obs} - A^{B}_{obs} \\ &= C^{S}_{sample} d \frac{z_{sample}}{z_{co\text{-}ion}} \cdot \left[-\mathrm{DMM} \cdot \varepsilon_{co\text{-}ion} \right. \\ &\quad \left. + (1-\mathrm{DMM}) \cdot \frac{z_{co\text{-}ion}}{z_{counterion}} \cdot \varepsilon_{counterion} \right] \end{aligned} \quad (11)$$

At a certain sample concentration and the charge ratio of the sample ion to the co-ion in a given electrophoretic system, the detectability of the sample ions is governed by the following inequalities, namely,

$$-\mathrm{DM}M \cdot \varepsilon_{co\text{-}ion} + (1-\mathrm{DMM}) \cdot \frac{z_{co\text{-}ion}}{z_{counterion}} \cdot \varepsilon_{counterion}$$

< 0 (normal displacement)

$$-\mathrm{DMM} \cdot \varepsilon_{co\text{-}ion} + (1-\mathrm{DMM}) \cdot \frac{z_{co\text{-}ion}}{z_{counterion}} \cdot \varepsilon_{counterion}$$

$= 0$ (no peak)

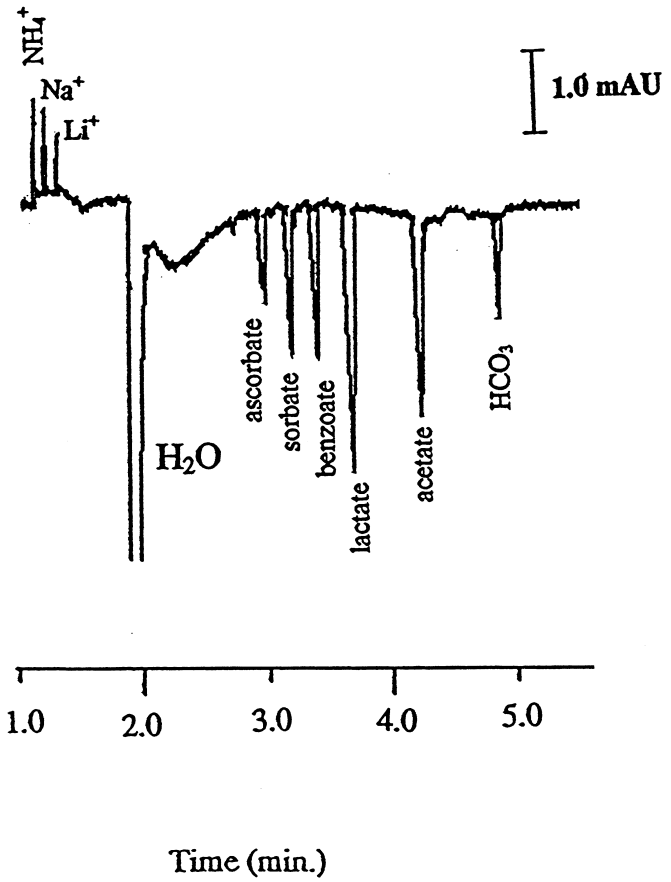

Fig. 6. Electropherogram of simultaneous separation of cations and anions in Tris (12.0 m*M*)/1,5-naphthalenedisulfonic acid (2.0 m*M*) BGE. pH=8.5; λ=224 nm; V=30.0 kV; capillary: 60 cm (total)×45 cm (effective). No reversal of the signal polarity for the detector was adopted for the present case.

$$-\mathrm{DMM}\cdot\varepsilon_{\text{co-ion}}+(1-\mathrm{DMM})\cdot\frac{z_{\text{co-ion}}}{z_{\text{counterion}}}\cdot\varepsilon_{\text{counterion}}$$

>0 (positive peak, absorbance increase)

By regrouping the parameters, we obtain the relationship of the molar absorptivity ratio of the co-ion to the counterion with the electrophoretic properties of the sample ions in the BGE, i.e.,

$$\frac{\varepsilon_{\text{co-ion}}}{\varepsilon_{\text{counterion}}}>\frac{(1-\mathrm{DMM})}{\mathrm{DMM}}\cdot\frac{z_{\text{co-ion}}}{z_{\text{counterion}}}$$ (normal displacement)

$$\frac{\varepsilon_{\text{co-ion}}}{\varepsilon_{\text{counterion}}}<\frac{(1-\mathrm{DMM})}{\mathrm{DMM}}\cdot\frac{z_{\text{co-ion}}}{z_{\text{counterion}}}$$

(positive peak, absorbance increase)

$$\frac{\varepsilon_{\text{co-ion}}}{\varepsilon_{\text{counterion}}}=\frac{(1-\mathrm{DMM})}{\mathrm{DMM}}\cdot\frac{z_{\text{co-ion}}}{z_{\text{counterion}}}$$ (no peak)

These inequalities indicate that the detection wavelength should be selected properly in order for all the sample ions to be detected as a normal peak of the indirect photometry. To see explicitly how much the molar absorptivity ratio influences the detectability of the sample ions, the term on the right-hand side of the inequalities given above were plotted against the

mobilities of the sample ions in different BGEs (cf. Table 2) as shown in Fig. 7. From Fig. 7, three regions could be identified, i.e.,

1. the region where $[(1-\mathrm{DMM})/\mathrm{DMM}](z_{\text{co-ion}}/z_{\text{counterion}})<0$;
2. the region where $[(1-\mathrm{DMM})/\mathrm{DMM}](z_{\text{co-ion}}/z_{\text{counterion}})=0$;
3. the region where $[(1-\mathrm{DMM})/\mathrm{DMM}](z_{\text{co-ion}}/z_{\text{counterion}})>0$.

These regions suggest that the selection of the detection wavelength is not critical for the proper detection of the sample ions with their mobilities equal to or less than that of the co-ion, because the molar absorptivity ratio is always a positive number, namely, $\varepsilon_{\text{co-ion}}/\varepsilon_{\text{counterion}}>0$. However, the selection of the detection wavelength is not arbitrary for the proper detection of the sample ions with their mobilities being larger than that of the co-ion. When the molar absorptivity ratio at a certain wavelength in a given BGE falls in the following region, namely,

$$0<\frac{\varepsilon_{\text{co-ion}}}{\varepsilon_{\text{counterion}}}\leq\frac{1-\mathrm{DMM}}{\mathrm{DMM}}\cdot\frac{z_{\text{co-ion}}}{z_{\text{counterion}}} \quad (12)$$

the sample ions will not be detected (no peak) or observed as a positive peak (absorbance increase). This phenomenon has been observed in several BGEs [23,30]. Fig. 8A shows one example of this observation for the separation of some cations and anions in 1,2-dimethylimidazole/sulfosalicylic acid BGE. The peak corresponding to K^+ in Fig. 8A shows that the detection wavelength used here is not appropriate for the present case. Fig. 8B shows the electropherogram of the same analytes in the same BGE but detected at a different wavelength. The peaks for all the cationic analytes are detected as normal displacement of their co-ion (1,2-di-

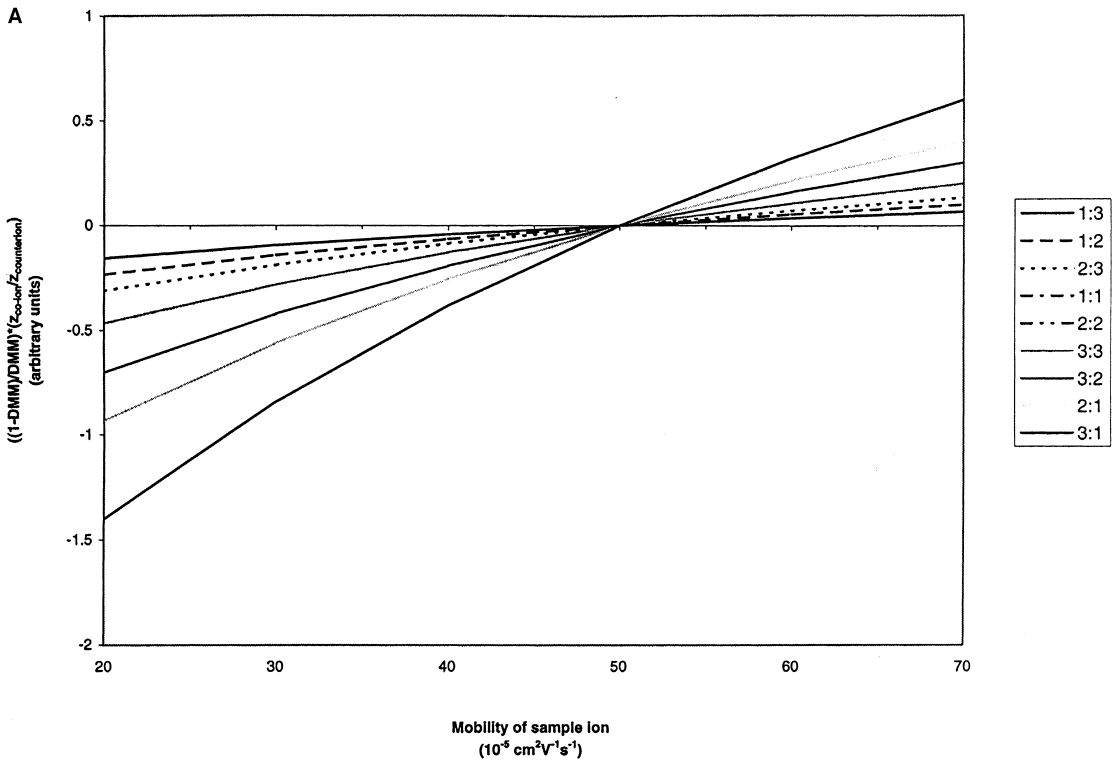

Fig. 7. Plot of $[(1-\mathrm{DMM})/\mathrm{DMM}]*[z(\text{co-ion})/z(\text{counterion})]$ against the effective mobilities of the sample ions in different BGEs (as given in Table 2). Charge ratios of co-ions to counterions ($z_{\text{co-ion}}/z_{\text{counterion}}$) are labelled in the figure. When the ($z_{\text{co-ion}}/z_{\text{counterion}}$) equals one, the profiles for the sample ions overlap.

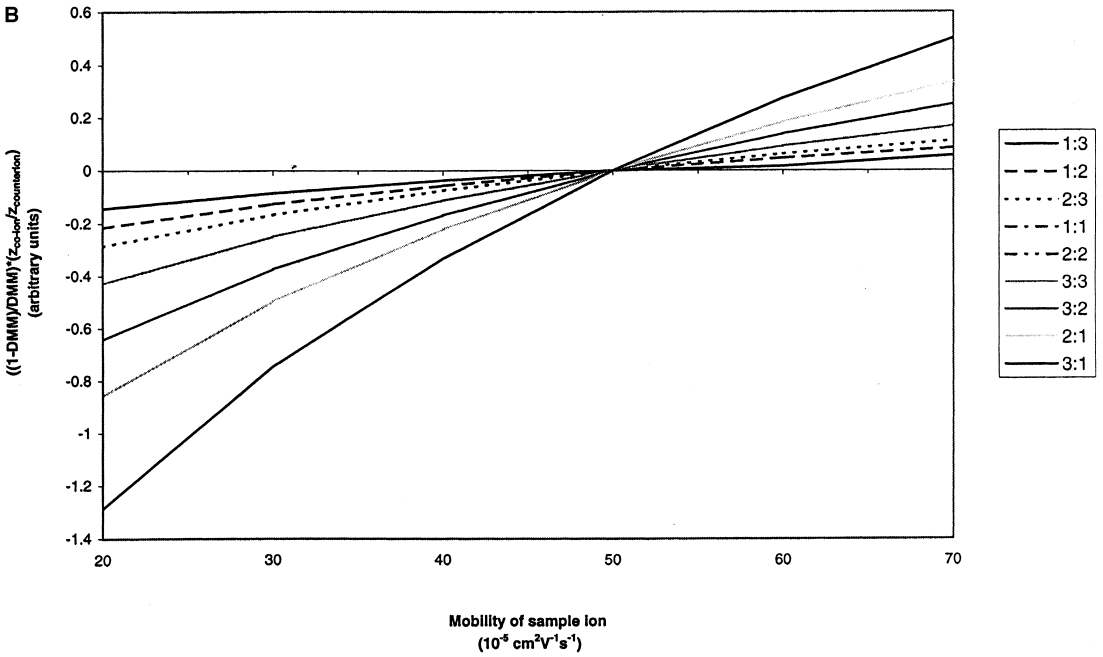

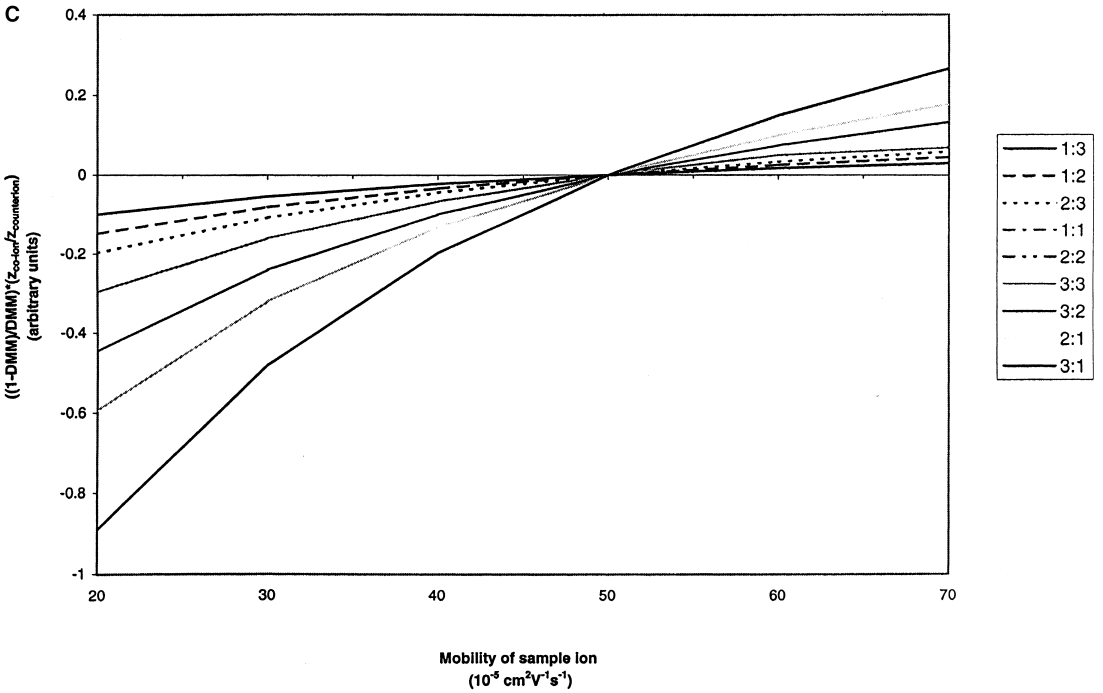

Fig. 7. (*continued*)

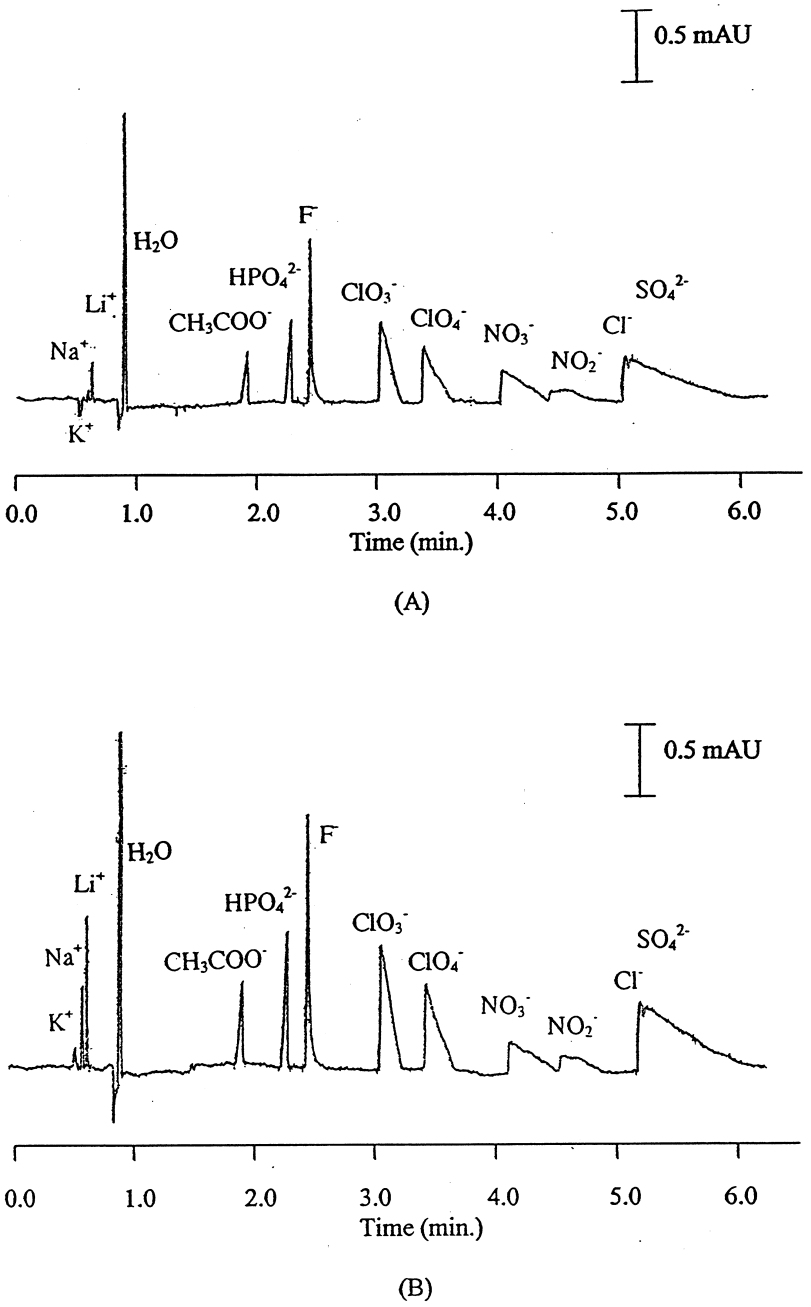

Fig. 8. Electropherogram of simultaneous separation of small cations and anions in two BGEs. (A) 1,2-dimethylimidazole (3.3 m*M*)/sulfosalicylic acid (0.87 m*M*) BGE at $\lambda = 226$ nm; (B) $\lambda = 217$ nm; (C) 1,2-dimethylimidazole (4.4 m*M*)/pyromellitic acid (0.68 m*M*) BGE at $\lambda = 210$ nm pH = 7.7; V = 29.0 kV.

methylimidazole) at this wavelength. By comparing the molar absorptivity ratios of the co-ion to counter-ion at these two wavelengths, it is found that the molar absorptivity ratio at 217 nm is larger than that at 226 nm. This is conceptually consistent with the theoretical prediction given above. However, the

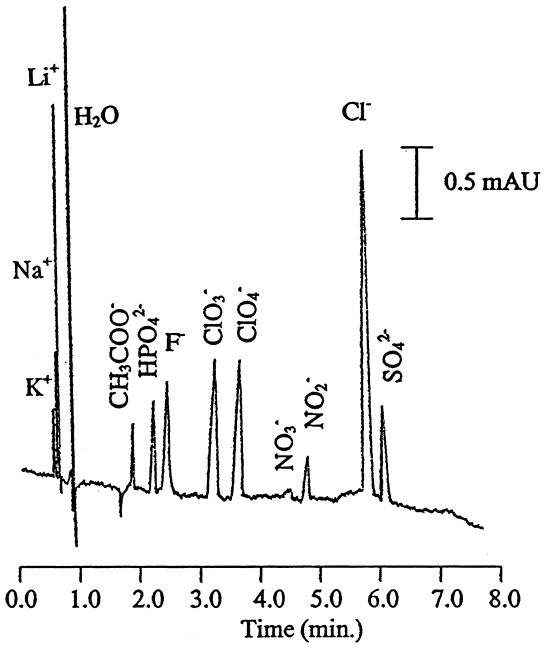

(C)

Fig. 8. (*continued*)

direct comparison of the terms in Eq. (12) is not consistent with the relationship described in Eq. (12) by using the data in Table 3 and effective mobilities in Fig. 8. The discrepancy observed here might be ascribed to the following two reasons. One is that the charge ratio of the co-ion to the counterion is not exactly known at the given pH. The other is that the effective mobilities of the co-ion and the counterion obtained in another buffer solution are not equivalent to those when they are used as the buffer solution itself. Nevertheless, the distorted peaks for the anionic analytes in Fig. 8A and 8B are attributed to the mismatch of the mobilities of the analytes and their co-ion (sulfosalicylate). In order to match well with the mobilities of these anionic ions, a co-ion with a faster mobility should be used to formulate the BGE according to the guidelines obtained before. Fig. 8C shows the electropherogram of the same analytes in the BGE of 1,2-dimethylimidazole/pyromellitic acid. From the peak shapes for all the anionic analytes, it can be concluded that the new BGE is matched better with the analytes than the one in Fig. 8A and 8B as compared to the mobilities of the two anionic co-ions in Table 3. To minimise the counteraction effect between the counterion and the co-ion in absorption, the detection would be carried out at the wavelength where the co-ion and the counterion have the equivalent molar absorptivities [31].

4.3.4. Method 4

Another way to detect the sample ions simultaneously is to use different wavelengths for the detection of different classes of sample ions. The purpose of using dual wavelengths is to decrease the positive effect of the UV-absorbing counterion on the absorption of the sample zones caused by displacement of the co-ion. In this case, the expression for the absorption of the sample zones is much like that for method 1. The constraints and guidelines for these two detection methods are quite similar. The detection wavelengths are selected at the individual maximum of the co-ion and the counterion with minimal overlapping of the absorption bands between them.

4.3.5. Method 5

In this detection method, the absorption of the sample zone is mainly dependent on the intrinsic absorptivity of the sample ion. The BGE will not directly influence the absorption of the sample zones, but strongly influence the shape and symmetry of the peaks. The constraints on proper formulation of BGE for this detection method have been discussed elsewhere [11,32].

5. Conclusion

The model developed in the present work provides much insight for the description of the relationship between sensitivity and electrophoretic properties of the BGEs. It describes satisfactorily the absorption of the sample zones in BGEs for indirect photometric detections. Rules extracted from the model can be used as guidelines for formulation of the BGEs for different detection methods. Although constraints on the selection of the detection conditions for the different detection methods are different, some rules extracted from the model for formulation of BGEs

are valid for all the detection methods. In order to increase the transfer ratios of the sample ions or to decrease the electromigration dispersion of the sample zones the mobility of the co-ion should be larger than or equal to that of the sample ions. Qualitative and semiquantitative information on the absorption of the sample zones in BGEs for the different detection methods can be extracted directly from the unified model.

Acknowledgements

Financial support from the National University of Singapore is gratefully acknowledged. The authors would like to thank Cecile Raguenes for her help in some experiments.

References

[1] M. Albin, P.D. Grossman, S.E. Moring, Anal. Chem. 65 (1993) 489A.
[2] J. Boden, K. Bächmann, J. Chromatogr. A 734 (1996) 319.
[3] F. Foret, S. Fanali, L. Ossicini, P. Boček, J. Chromatogr. 470 (1989) 299.
[4] M.W.F. Nielen, J. Chromatogr. 588 (1991) 321.
[5] G.J.M. Bruin, A.C. Van Asten, X. Xu, H. Poppe, J. Chromatogr. 608 (1992) 97.
[6] W. Buchberger, S.M. Cousins, P.R. Haddad, Trends Anal. Chem. 13 (1994) 313.
[7] J. Collet, P. Gareil, J. Chromatogr. A 716 (1995) 115.
[8] F. Steiner, W. Beck, H. Engelhardt, J. Chromatogr. A 738 (1996) 11.
[9] S. Motellier, K. Gurdale, H. Pitsch, J. Chromatogr. A 770 (1997) 311.
[10] J.L. Beckers, J. Chromatogr. A 764 (1997) 111.
[11] V. Sustacek, F. Foret, P. Boček, J. Chromatogr. 545 (1991) 239.
[12] E.S. Yeung, Acc. Chem. Res. 22 (1989) 125.
[13] P. Doble, P. Andersson, P.R. Haddad, J. Chromatogr. A 770 (1997) 291.
[14] S.M. Cousins, P.R. Haddad, W. Buchberger, J. Chromatogr. A 671 (1994) 397.
[15] F.E.P. Mikkers, F.M. Everaerts, Th.P.E.M. Verheggen, J. Chromatogr. 169 (1979) 1.
[16] F. Kohlrausch, Ann. Phys. Chem. 62 (1897) 209.
[17] H. Poppe, Anal. Chem. 64 (1992) 1908.
[18] M. Macka, P. Andersson, P.R. Haddad, Anal. Chem. 70 (1998) 743.
[19] X. Xu, W.Th. Kok, H. Poppe, J. Chromatogr. A 742 (1996) 211.
[20] E.S. Yeung, W.G. Kuhr, Anal. Chem. 63 (1991) 275A.
[21] R.L. St. Clair III, Anal. Chem. 68 (1996) 569R.
[22] Y.H. Lee, T.I. Lim, J. Chromatogr. A 675 (1994) 227.
[23] X. Xiong, S.F.Y. Li, J. Chromatogr. A 822 (1998) 125.
[24] P. Kuban, B. Karlberg, Anal. Chem. 70 (1998) 360.
[25] A.E. Martell (Ed.), Stability Constants of Metal-Ion Complexes, Chemical Society, London, 1964, p. 595.
[26] R.M. Smith, A.E. Martell (Eds.), Critical Stability Constants, Vol. 6, 2nd supplement, Plenum, New York, 1989, p. 250.
[27] J.A. Dean (Ed.), Lange's Handbook of Chemistry, McGraw-Hill, New York, 1985.
[28] M.T. Ackermans, F.M. Everaerts, J.L. Beckers, J. Chromatogr. 549 (1991) 345.
[29] B. Lu, D. Westerlund, Electrophoresis 19 (1998) 1683.
[30] X. Xiong, S.F.Y. Li, Electrophoresis 19 (1998) 2243.
[31] S.A. Shamsi, N.D. Danielson, Anal. Chem. 67 (1995) 4210.
[32] J. Bullock, J. Strasters, J. Snider, Anal. Chem. 67 (1995) 3246.